Hindawi
Journal of Nanomaterials
Volume 2019, Article ID 3484239, 11 pages
https://doi.org/10.1155/2019/3484239

Research Article

Development of a Transparent Coating to Enhance Self-Cleaning Capability and Strength in Conventional Paper

Xiangdong Ye, Junwen Hou, Xuerui Yan, and Xiaojun Wu

School of Mechanical and Electrical Engineering, Shaanxi Key Laboratory of Nano Materials and Technology, Xi'an University of Architecture and Technology, Xi'an 710055, China

Correspondence should be addressed to Xiangdong Ye; yexiangd@xauat.edu.cn

Received 1 June 2019; Revised 7 July 2019; Accepted 26 July 2019; Published 9 September 2019

Academic Editor: Ashok K. Sundramoorthy

Paper is one of the most widely used materials, due to its application in books, packaging, and office supplies. However, conventional paper has many disadvantages, such as low tensile strength, poor resistance to water and oil contamination, lack of antigraffiti capability, and easily deformed by moisture. Therefore, we proposed a double-layer protective coating that consists of a polyurethane (PU) bottom layer, to enhance tensile strength, and a top polydimethylsiloxane (PDMS) composite layer to enable antigraffiti and contamination-resistant capabilities. In the study, a double-layer coating was applied to conventional paper, using a simple two-step spraying method. The results showed that the prepared coating structure exhibited outstanding self-cleaning characteristics with respect to both water and oil contamination and adequately demonstrated antigraffiti capability. Moreover, the coating maintained superhydrophobic and oil-stain resistance after four months of outdoor storage. Finally, the tensile strength of the coated paper was 6.3 times as high as that of the original paper, making this coating structure a promising solution to the problems that limit paper from being more widely utilized in commercial and consumer application.

1. Introduction

Paper is a widely used material throughout numerous commercial industries and by individual consumers, owing to its versatility, low cost, extensive production, and short processing time. However, despite the high demand, paper use is somewhat limited due to the following factors: (1) paper is composed of countless fibers that are inconsistently applied. Due to variations in fiber size and arrangement, copious gaps develop between the fibers. As such, when paper comes in contact with water, the water molecules are absorbed along the gaps, making it vulnerable to moisture and difficult to preserve over long periods of time [1]. (2) Paper is easily smudged by oily materials because of its poor antigraffiti performance. (3) Paper has a low tensile strength and is therefore susceptible to tearing. For these reasons, researchers have attempted to design a superhydrophobic coating that is self-cleaning, dust-proof, moisture-proof, and anticorrosion [2–5]. Examples of such studies include Ogihara et al. [6], who reported that superhydrophobic coatings can be deposited on paper by spraying alcohol suspensions of SiO_2 nanoparticles; Baidya et al. [7] described a simplistic methodology to develop a superhydrophobic paper via manufacture of fluoroalkyl functionalized cellulose nanofibers (CNFs); Shi et al. [8] prepared a superhydrophobic nanocomposite coating using hydrophobic silica nanoparticles as a filter and polyvinylidene fluoride (PVDF) as a film-forming material, which was applied to the paper's surface through a simple, one-step spray dispersion method; Wang et al. [9] manufactured a superhydrophobic paper by coating it with silica sol using tetraethylorthosilicate (TEOS) and trimethylethoxysilane (TMES) as a precursor and coprecursor, respectively. However, the superhydrophobic coatings prepared by the above methods are lacking resistance to oily substances and thus do not have a self-cleaning effect [10].

Because the results of these earlier attempts to develop superhydrophobic coatings do not fully protect the paper, alternative solutions continue to be investigated. Dimitrakellis et al. [11] prepared superhydrophobic

and, to some degree, oleophobic paper surfaces by using atmospheric pressure plasma etching. Zhong et al. [12] reported a novel antismudge coating, cured by natural sunlight exposure or 35 sec of UV irradiation. Zheng et al. [13] developed an NP-GLIDE coating that requires 5 min of irradiation to yield a transparent glaze with antismudge properties. Wu et al. [14] developed a strategy for preparing smooth antismudge coatings; the resultant coating is dried in a desiccator under a gentle nitrogen flow for 20 min, then a curing procedure is performed at 140°C for 1 hr. Rabnawaz and Liu [15] reported an antifouling coating, several tens of microns thick, that was prepared from commercial precursors using a graft copolymer-based method. This coating can be used on many substrates including paper.

Another method of preventing paper from being damaged by water- and/or oil-based substances consists of preparing superamphiphobic paper via plasma processing [16, 17], vapor deposition [18, 19], or sprayed fluorinated silicon dioxide [20, 21]. However, the required etching in plasma processing can cause irreparable damage to the paper's surface, while vapor deposition and spraying fluorinated silica particles generate superamphiphobic properties by covering the opaque functional coating on the paper surface. Subsequently, the paper surface will become opaque, thus affecting any existing information on the paper's surface. PDMS is a widely used and environmental-friendly polymer due to its low cost, high transmittance, and low surface energy. Utilizing the advantages of PDMS, Sahoo et al. [22] prepared a novel self-cleaning polymer composite with self-healing ability after chemical and mechanical damage. Yang et al. [23] reported the superhydrophobic coatings based on PDMS and TiO_2-NPs. Due to the photocatalytic property of TiO_2-NPs, the PDMS/TiO_2-NP coatings could remove the organic pollutes efficiently and showed excellent self-cleaning properties. Furthermore, none of the coatings discussed thus far will increase the paper strength, so the paper can still be easily torn or damaged from multiple external factors.

In an attempt to mitigate the shortcomings of conventional paper, we propose a double-layer protective coating composed of a PU bottom layer and a PDMS top composite layer. When the coating was applied to the paper with a simple two-step spraying process, it was shown to be self-cleaning and transparent and has high antigraffiti performance and enhanced strength.

2. Experimental

2.1. Materials and Instruments. Deli Co. provided 7465 copy paper. The 98% AR toluene, 5 μm diameter polytetrafluoroethylene (PTFE), and 16–25 nm diameter hydrophobic silica were provided by Macklin Co., while the 98% AR hexadecane was procured from Aladdin Co. 1H- and 2H-perfluorodecyltrimethoxysilane were purchased from Silworld Chemical Co. All three chemical companies are based in China. Single component ADEKIT P 4202 PU, ESSIL 291 PDMS, and the curing agent were supplied by Axson Co. in the United States. Oil and carbon black are purchased from local distributors. All reagents were used as received without further purification.

A 524 G magnetic stirrer, produced by the Shanghai Mei Ying Pu Instrument Manufacturing Co., and a 500 W ultrasonic vibrator, manufactured by Hangzhou Frante Ultrasound Technology Co., were used to disperse the solution. A W71, ANEST IWATA Corporation, spray gun was employed for solution spraying. A Japan Hitachi Group S3000 scanning electron microscope (SEM) and a BX53M Olympus Corporation light microscope were used for surface topography characterization. An atomic force microscope was used to detect physical morphology (Bruker Dimension Icon, Brook) with HQ-300-Au (Ti/Au Coated Tips, 40 N/m, 300 kHz). The water contact angles (CAs) on all the surfaces were measured using the JC2000C1 contact angle measurements system—manufactured by Shanghai Zhongchen Digital Equipment. Olympus Corporation LEXT OLS4000 3D Measuring Laser Microscope is used to measure the thickness of coatings. A UTM2203, 0-5000N series Single Column Computerized Electronic Universal Testing Machine, produced by Zhenbang Testing Machinery Factory, was used for tensile strength analysis.

2.2. Preparation of Paper with PU Strength Layer. Ten milliliters of PU was added to the spraying device and sprayed on the paper's surface for 6 sec at a distance of 30 cm. The coating was then left to cure at room temperature for 4 hr, or heated at 80°C for 20 min, to reach a semicured state.

2.3. Preparation of Paper with PDMS Composite Layer. Zero point two grams of SiO_2 was mixed with 10 ml of toluene reagent and sonicated for 10 min. Next, 0.05 g of PTFE particles was added and the solution was sonicated for an additional 20 min to form a uniform dispersion. One gram PDMS and 0.1 g curing agent were mixed into the solution, which was magnetically stirred for 10 min. The mixture was then set aside and designated Solution A. Next, Solution B was composed by mixing 1 ml perfluorodecyltrimethoxysilane with 10 ml alcohol and magnetically stirred for 20 min.

Solution A was sprayed on the semicuring PU strength coating for 6 sec at a distance of 30 cm. The coating layer was left to cure at room temperature for 4 hr, or heated at 80°C for 20 min, to reach a semicured state. Next, Solution B was sprayed on the semicuring Solution A layer for 3 sec at a distance of 30 cm. Curing was then resumed either at room temperature for 20 hr, or by heating at 80°C for 1.5 hr, to fully cure the coatings on the paper.

3. Results and Discussion

3.1. Topography Characterization and EDS Analysis. Figures 1(a) and 1(b) depict the paper before and after being sprayed with the prepared coating. Visual comparison of the two photographs shows almost no difference in the appearance of the paper. The samples were also analyzed by an optical microscope and SEM. Results are shown in Figures 1(c) and 1(d), respectively.

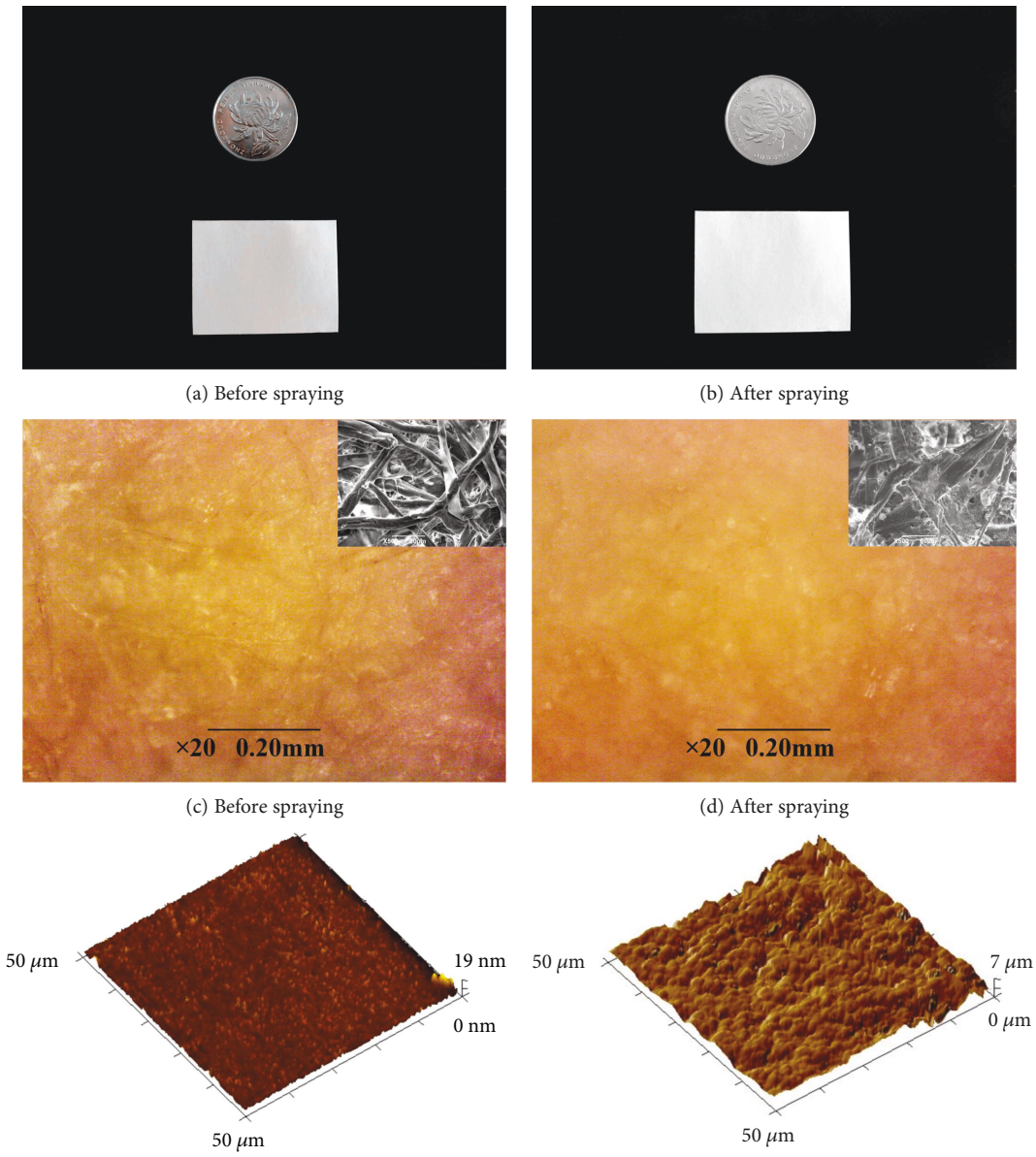

(a) Before spraying

(b) After spraying

(c) Before spraying

(d) After spraying

(e) Before spraying

(f) After spraying

Figure 1: Continued.

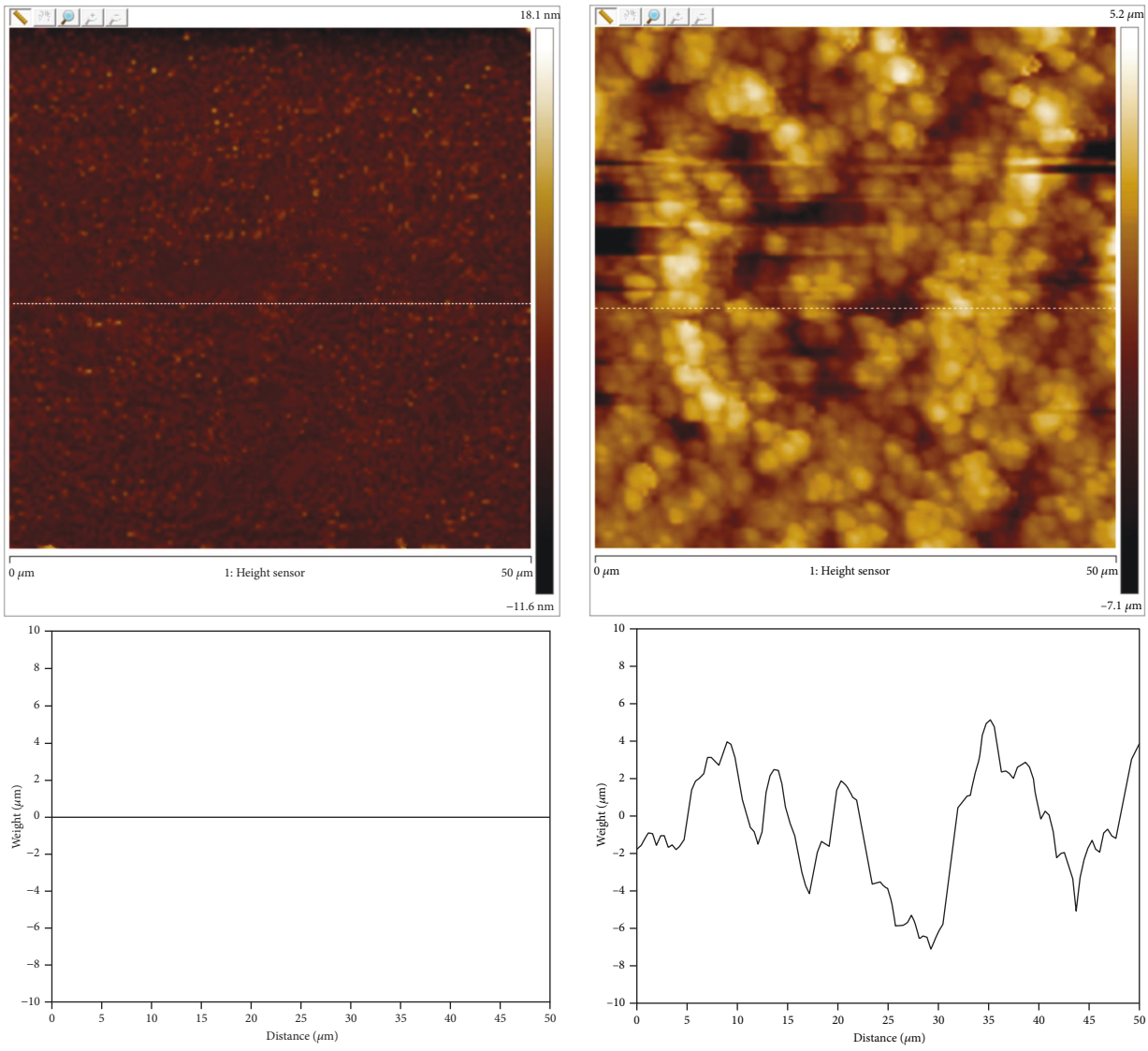

(g) Before spraying (h) After spraying

Figure 1: Images of paper pattern before and after spraying: (a) photograph before spraying, (b) photograph after spraying, (c) optical microscope and SEM before spraying, (d) optical microscope and SEM after spraying, (e) AFM image of coating before spraying, (f) AFM image of coating after spraying, (g) height profile of coating before spraying, and (h) height profile of coating after spraying.

Figure 1(c) shows the paper sample before being sprayed with the prepared coating. Notice that the fibers are irregularly stacked, with numerous and varied size voids throughout. Furthermore, the surface of individual fibers is relatively smooth. Figure 1(d) depicts the paper after being sprayed with the coating. In contrast to Figure 1(c), the gaps between the fibers are filled in and the individual fibers demonstrate a rough and uneven texture. Moreover, the surface morphology of the glass substrate before and after the coating spraying is measured by the AFM as shown in Figures 1(e)–1(h), respectively. According to the data of AFM, the Ra before spraying is 3.3 nm, and after spraying, Ra becomes 1.0 μm. Comparing Figures 1(e) and 1(g) with Figures 1(f) and 1(h), it is apparent that the sprayed coating will make the substrate much rough and uneven.

In addition, EDS analysis was carried out to detect any changes in element composition and/or concentration between the "before" and "after" samples. The experimental results are shown in Figure 2.

Figure 2(a) shows that the original sample was comprised exclusively of carbon and oxygen, with relative concentrations of 67.75% and 32.25%, respectively. After the coating was applied, the elemental composition of the paper's surface included silicon, carbon, oxygen, and fluorine, in relative concentrations of 35.21%, 31.18%, 29.62%, and 3.99%, respectively (Figure 2(b)). Thus, three major changes took place when the coating was applied: (1) silicon and fluorine were added, (2) silicon, instead of carbon, displayed the highest concentration, and (3) the relative concentrations of both carbon and oxygen decreased in comparison to the uncoated sample.

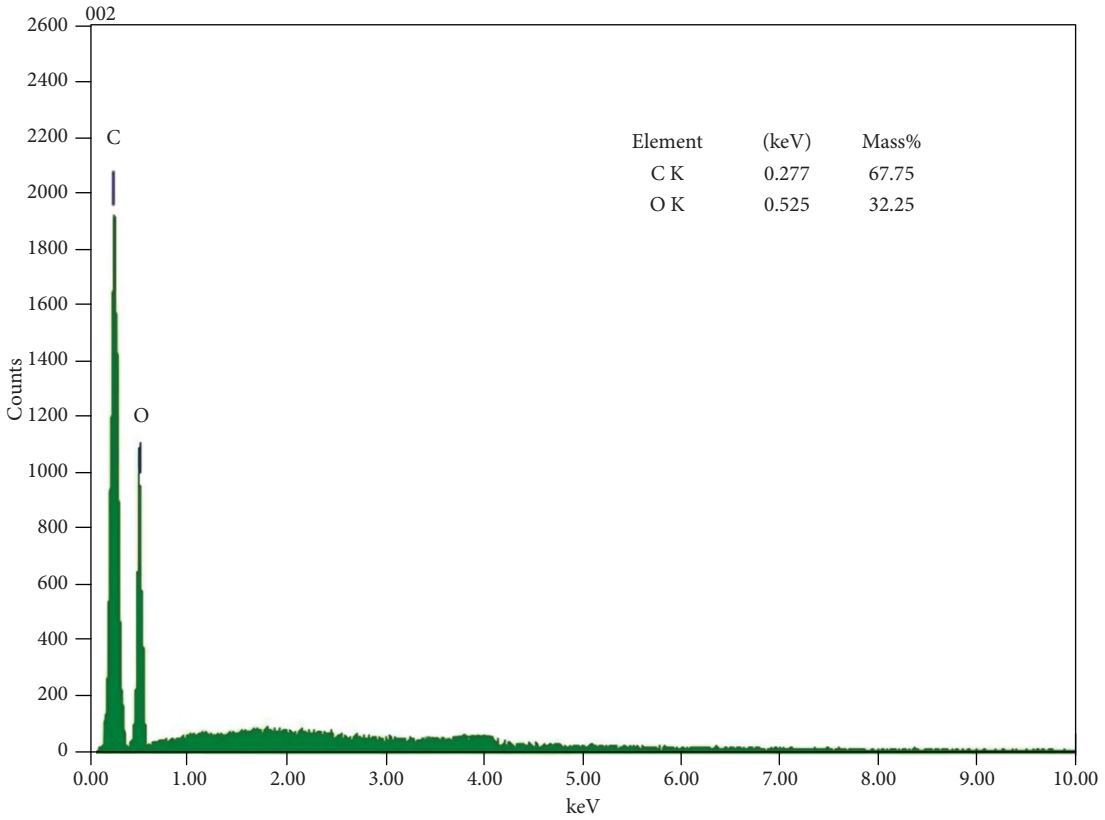

(a) Before application of the coating

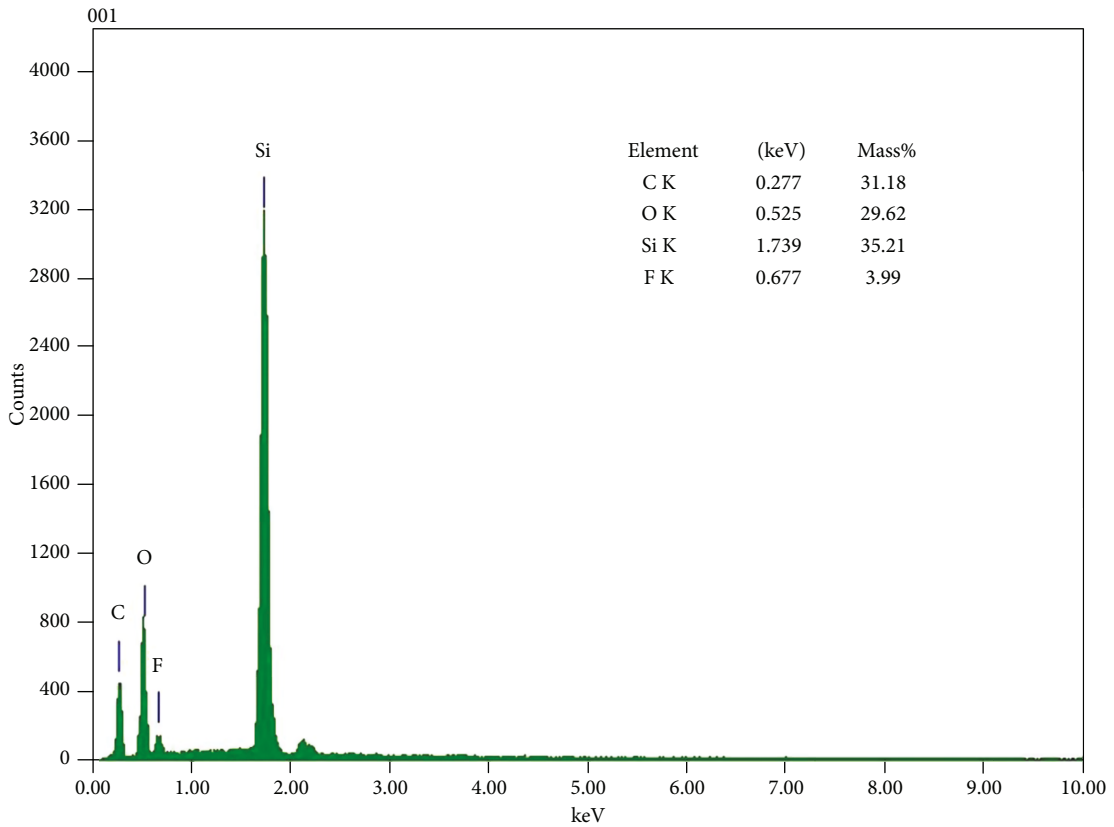

(b) After application of the coating

Figure 2: EDS elemental analysis of the paper sample before and after coating application.

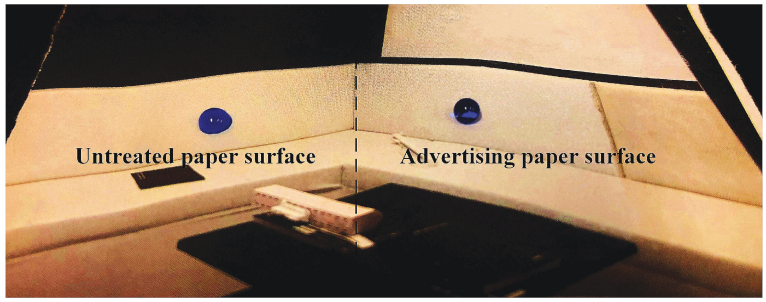

Figure 3: Water droplets on the original paper and coated paper samples.

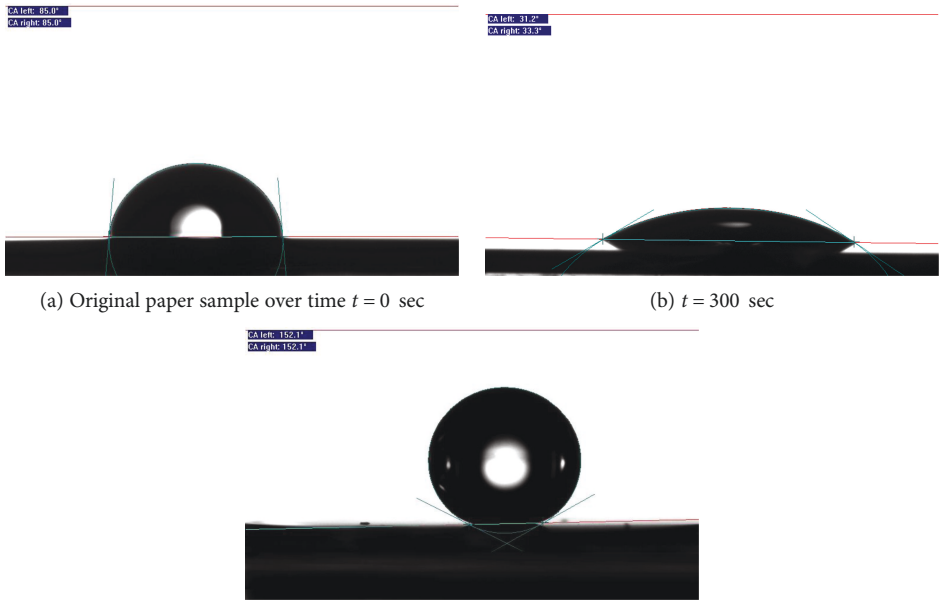

(a) Original paper sample over time $t = 0$ sec

(b) $t = 300$ sec

(c) Paper sample with coating of Solution A

Figure 4: Contact angle images of water drops on the original sample and the sample with Solution A coating.

3.2. Wettability of the Original Sample vs. the Sample Coated with Solution A. A water drop test, employing blue pigmented water, was used to assess the wettability of the original sample and a paper sample coated with Solution A (Figure 3).

The water drop on the original sample was hemispherical in shape and over time absorbed into the paper, causing the paper to become damp and deformed. Contrarily, the water drop on the paper with Solution A coating was spherical in shape, and no water was absorbed over time. These results were quantified using CA measurements, which are shown in Figure 4.

Figure 4(a) shows the initial water CA of the original sample to be 85°, which indicates a weak hydrophilicity. However, after 300 sec, the contact angle decreased to 31.2°, as shown in Figure 4(b). In contrast, the water CA of the paper sample coated with Solution A was initially 152.1° and remained superhydrophobic over time (Figure 4(c)).

To gain further insight into the effects of PDMS, PTFE, and SiO_2 on coating wettability, the three Solution A components were individually investigated and the results are shown in Table 1.

Table 1: Effects of Solution A components—PDMS, PTFE, and SiO_2—on the coating wettability (in 10 ml toluene).

Coating	PDMS (g)	PTFE (g)	SiO_2 (g)	Contact angle (°)
Original paper	0	0	0	85.0
A_1	1	0	0	117.5
A_2	1	0.05	0	130.8
A_3	1	0	0.2	140.3
A	1	0.05	0.2	152.1

Based on the results in Table 1, it is clear that surface coating wettability was affected by the addition of PDMS, SiO_2, and PTFE. With the addition of PDMS, the wettability of coating A_1 changed from weak hydrophilic to hydrophobic and the CA increased from 85° to 117.5°. The

Figure 5: Effects of antigraffiti on paper with two coatings.

Table 2: Antigraffiti effect of paper with different coatings.

Coating	Solution B spraying	Superhydrophobic	Antigraffiti effect
A_1	No	No	No
A_2	No	No	No
A_3	No	No	No
A	No	Yes	No
A_1B	Yes	No	No
A_2B	Yes	No	No
A_3B	Yes	No	No
AB	Yes	Yes	Yes

subsequent addition of PTFE micron particles improved the micro roughness of coating A_2, generating a further increase in the CA to 130.8°. When the PTFE micron particles were replaced by SiO_2 nanoparticles, the augmented irregular nanostructures of coating A_3 improved the CA some more, bringing it up to 140.3°. Finally, under the combined action of PDMS, SiO_2 nanoparticles, and PTFE micron particles, coating A became superhydrophobic with a CA of 152.1° due to the formation of micro-nanocomposite structures.

3.3. Characterization of the Paper Coating Antismudge Capability. Graffiti damage is a major problem in cities throughout the world, so there is value of investigating and understanding the antigraffiti properties of paper. Thus, the antismudge capability of our paper coatings was investigated and the results are shown in Figure 5.

Figure 5 depicts an entire paper sample that was coated with Solution A; an additional coating of Solution B was applied within the small, inset dotted frame. The area coated with only the Solution A shows clear evidence of being smudged by a marker, while the area coated with both Solutions A and B (PDMS composite coatings) demonstrates antigraffiti properties.

The antigraffiti capability was further characterized by examining coatings of varied compositions and properties. The results from this investigation are depicted in Table 2.

As shown in Table 2, none of the coatings composed exclusively of Solution A depicted an antigraffiti effect, which demonstrates that Solution B is required to enable antigraffiti capability. Among the coatings comprised of both Solutions A and B, the only one characterized by antigraffiti capability was generated by spraying Solution B directly on top of one Solution A layer (PDMS composite coatings). These results indicate that in a highly hydrophobic material, the introduction of low-energy materials will provide the surface with antigraffiti properties.

3.4. Resistance of the PDMS Composite Layer to Oil Contamination. In this experiment, a mixture of oil and carbon black was used to simulate oil contamination. The mixture was dropped onto the surface of the original paper and the paper coated with a PDMS composite coating. The process was videotaped from start to finish and Figure 6 reflects different stages throughout the experiment that were isolated from the video.

As shown in Figures 6(a)–6(c), when oil was dropped on the original paper, it soaked into the surface and was unable to drop down and roll off. As a result, the paper exhibited oil staining and blot. However, Figures 6(d)–6(f) show that when oil was dropped on the paper with a PDMS composite coating, it quickly rolled off the paper's surface and left no trace of oil staining.

3.5. Tensile Strength of Coated Paper. The application of paper is limited because its low tensile strength allows it to be easily torn or damaged. In order to improve the strength of conventional paper, a PU strength coating layer was added between the PDMS composite layer on top and the paper on the bottom. Figure 7 depicts the complete proposed structure of the paper and coatings.

Moreover, LEXT 3D Measuring Laser Microscope was used to measure the thickness of the whole coating (PDMS composite and PU strength layer). Make the coating into a step pattern and measure the height of the step, and one of the measurements is shown in Figure 8.

The results in Figure 8 show that the coating thickness on paper surface is about 6.6 μm. The average of five measurements on different positions is taken as the final thickness of the coating, and the average thickness of the coating was 6.8 μm.

In order to test the tensile strength of the paper, both with and without coatings, the paper samples were cut into 10 mm × 50 mm rectangular strips. The cut samples were clamped on a single-column universal testing machine and stretched at a uniform speed of 0.1 mm/min. The results are shown in Figure 9.

Figure 9 shows 1.1 MPa as the maximum stress of the original, uncoated paper and demonstrates that it will completely rupture after 840 sec. The maximum stress of the PDMS composite-coated paper is 2.1 MPa, and it will tear completely after 2000 sec. However, the maximum stress of the paper covered with both PDMS composite coating and PU strength coating was 6.9 MPa, ~6.3 times as high as that of the original paper.

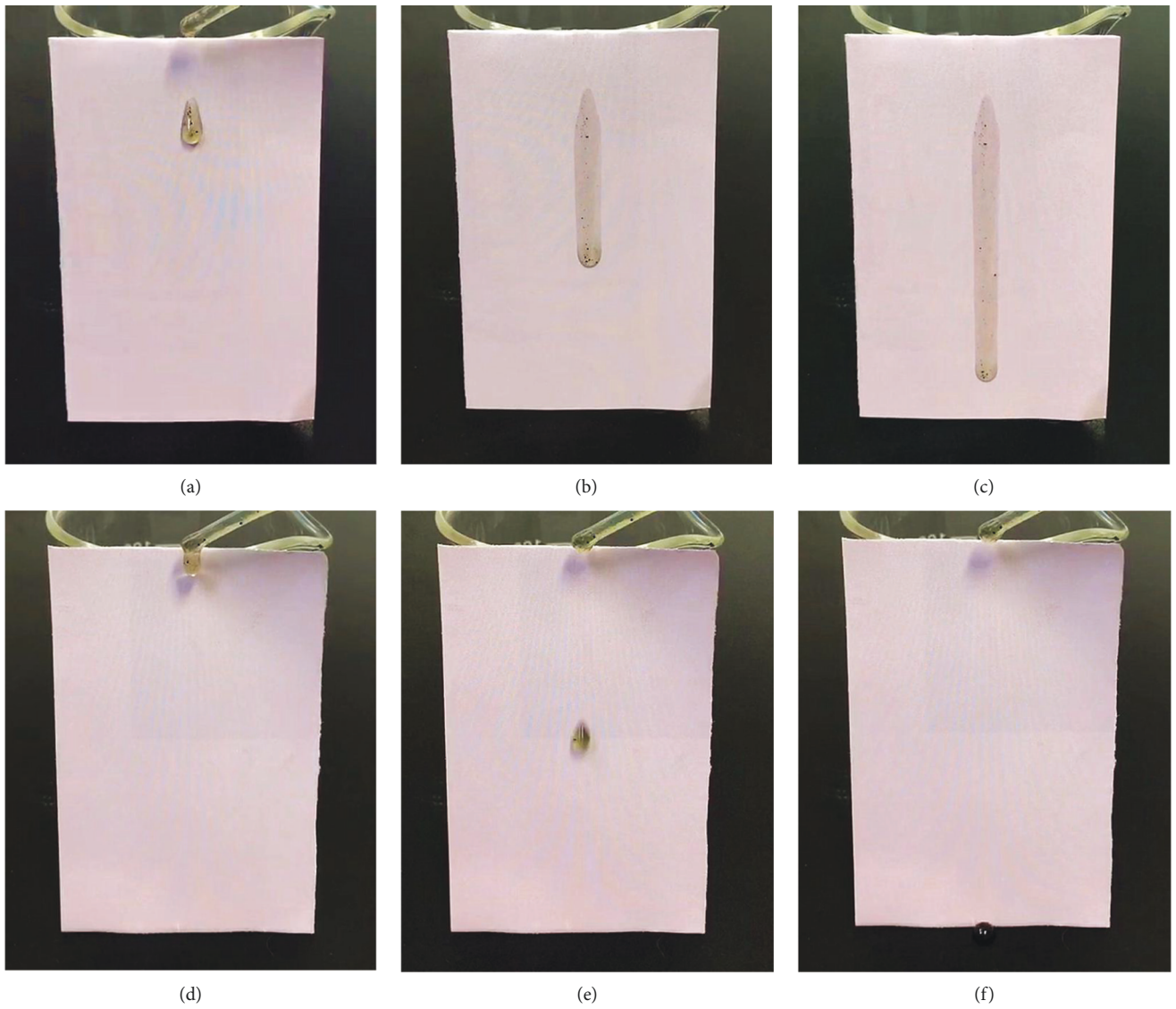

Figure 6: Photos of oil contamination dropped on the original paper: (a) $t = 0$ sec; (b) $t = 10$ sec; (c) $t = 60$ sec. Photos of oil contamination dropped on the paper with PDMS composite coating: (d) $t = 0$ sec; (e) $t = 0.3$ sec; (f) $t = 1$ sec.

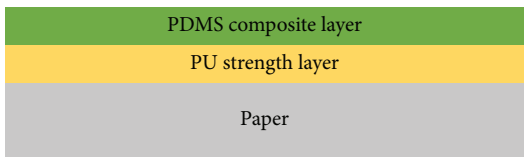

Figure 7: Complete structure of the double-layer coating.

3.6. Coating Transmittance. The transmittance of the entire coated structure, including the PDMS composite coating and the PU strengthener coating, was inspected on glass using an ultraviolet-visible spectrophotometer. Results are shown in Figure 10.

The maximum transmittance of the bare glass was 91.19% in the visible wavelength range of 350-800 nm, while the maximum transmittance of the glass with the entire coating structure was ~70% in the visible wavelength range. These results indicate that the coatings have adequate transmittance for message expression on paper.

3.7. Wear Resistance of Coatings. The coatings weighing 200 g were placed facedown on a sandpaper with 800 meshes and pushed back and forth for 10 cm, which is a cycle. After each cycle, the contact angle is measured and the testing results are shown in Figure 11.

The testing results show that after 10 abrasion cycles, the coating still keeps superhydrophobic and resistance to oil contamination, indicating that the coating has the outstanding wear-resistant property.

3.8. Durability of the Coatings. To determine the durability of these manufactured paper coatings, the paper sample was covered with the entire coating structure and placed in an

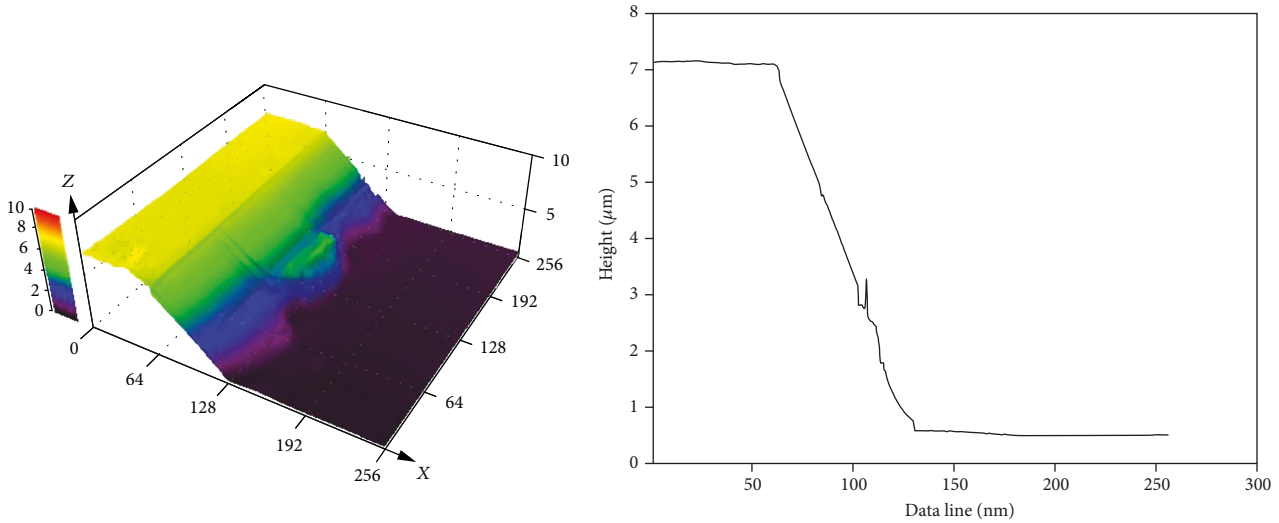

Figure 8: Measurement of coating thickness.

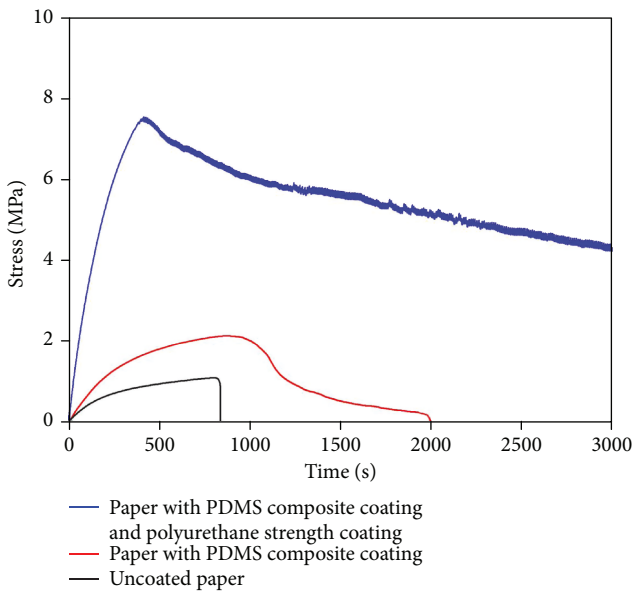

Figure 9: Relationship between tensile strength and time of the three kinds of paper.

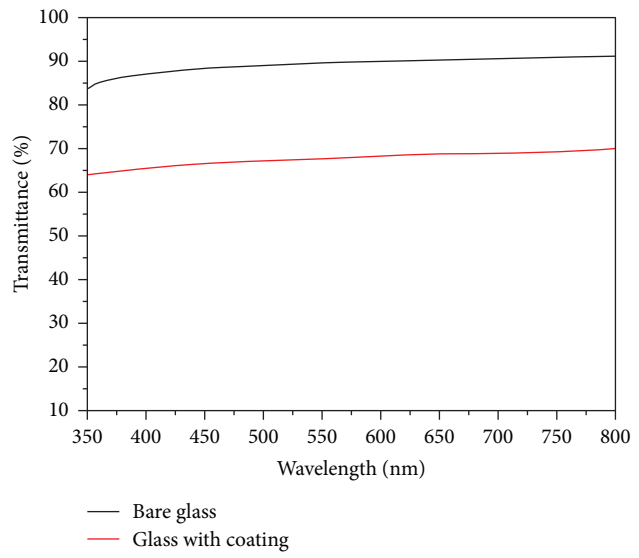

Figure 10: Transmittance on bare glass and on glass with whole coatings.

outdoor environment. The durability of the coating was determined by measuring the static water and hexadecane CAs once a month for four months. CA results are depicted in Figure 12.

Figure 12 shows that the coating CAs both decreased slightly with time. However, the water CA remained at ~150° demonstrating superhydrophobicity, and the hexadecane CA remained above 50°, indicating that the coating is characterized by good resistance to contamination over time.

4. Conclusions

In this study, a transparent multifunctional double layer was prepared and applied to paper using a simple two-step spraying process that implemented PU as a strength layer and composite PDMS as an anticontamination layer. The coating structure changed the paper's properties, so that it was no longer easily deformed by moisture, contaminated by graffiti and/or oil, or effortlessly torn. Compared with similar studies, PU and PDMS are used as the main materials as the strength layer and the antigraffiti functional layer, respectively. These two materials have low cost, nontoxicity, simple process, and good light transmittance. The coated paper has good self-cleaning properties with respect to both water and oil contamination and adequate antigraffiti capability. Moreover, the coating still maintained self-cleaning properties after four months of outdoor storage. Finally, the tensile strength of the coated paper is 6.3 times as high as that of

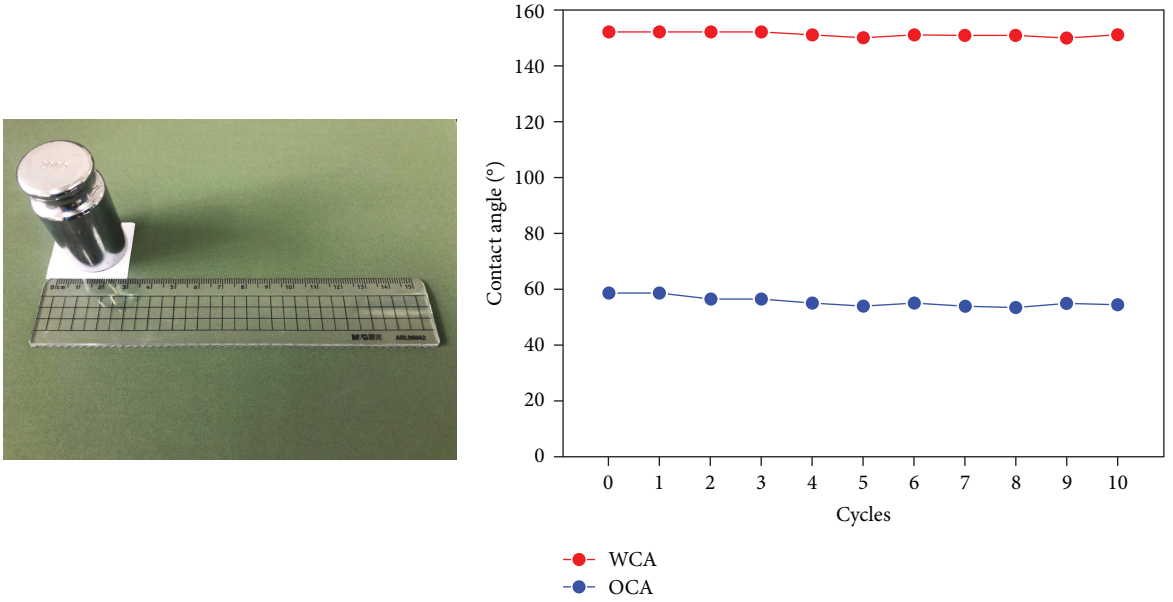

Figure 11: The wear-resistant test process device; water/oil CA as a function of the number of abrasion cycles for coatings.

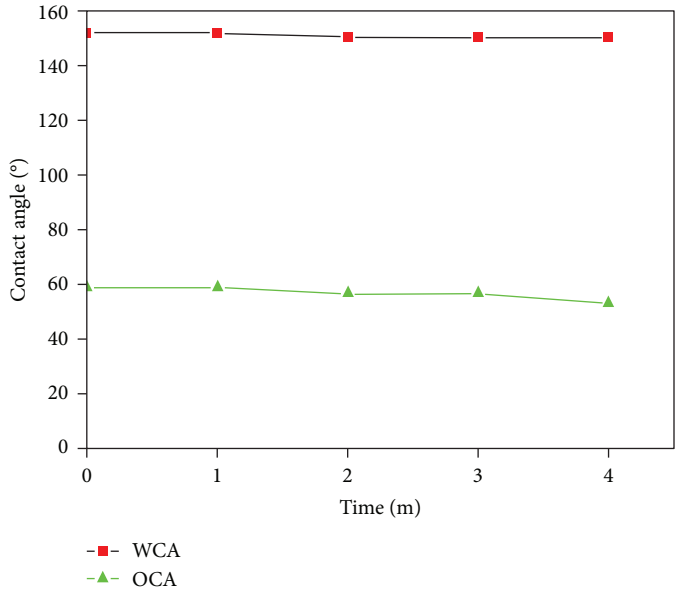

Figure 12: Changes in water and hexadecane on the coated paper over time.

the original paper sample; and thus, the coating structure should be potentially considered for expanding paper's application in commercial industry.

Data Availability

The data used to support the findings of this study are available from the corresponding author upon request.

Conflicts of Interest

The authors declare that they have no conflicts of interest.

Acknowledgments

This work was funded by the National Natural Science Foundation of China (Grant No. 51475353), the Natural Science Basic Research Program of Shaanxi Province (Grant No. 2016JM5004), and the Key Laboratory of the Shaanxi Provincial Department of Education (Grant No. 16JS057).

References

[1] Q. Wen, F. Guo, F. Yang, and Z. Guo, "Green fabrication of coloured superhydrophobic paper from native cotton

cellulose," *Journal of Colloid and Interface Science*, vol. 497, pp. 284–289, 2017.

[2] J. T. Simpson, S. R. Hunter, and T. Aytug, "Superhydrophobic materials and coatings: a review," *Reports on Progress in Physics*, vol. 78, no. 8, article 086501, 2015.

[3] S. Yu, Z. Guo, and W. Liu, "Biomimetic transparent and superhydrophobic coatings: from nature and beyond nature," *Chemical Communications*, vol. 51, no. 10, pp. 1775–1794, 2015.

[4] M. R. Karim and M. S. Islam, "Thermal behavior with mechanical property of fluorinated silane functionalized superhydrophobic pullulan/poly (vinyl alcohol) blends by electrospinning method," *Journal of Nanomaterials*, vol. 2011, Article ID 979458, 7 pages, 2011.

[5] F. F. Chen, Y. J. Zhu, Z. C. Xiong, T. W. Sun, and Y. Q. Shen, "Highly flexible superhydrophobic and fire-resistant layered inorganic paper," *ACS Applied Materials & Interfaces*, vol. 8, no. 50, pp. 34715–34724, 2016.

[6] H. Ogihara, J. Xie, J. Okagaki, and T. Saji, "Simple method for preparing superhydrophobic paper: spray-deposited hydrophobic silica nanoparticle coatings exhibit high water-repellency and transparency," *Langmuir*, vol. 28, no. 10, pp. 4605–4608, 2012.

[7] A. Baidya, M. A. Ganayee, S. Jakka Ravindran et al., "Organic solvent-free fabrication of durable and multifunctional superhydrophobic paper from waterborne fluorinated cellulose nanofiber building blocks," *ACS Nano*, vol. 11, no. 11, pp. 11091–11099, 2017.

[8] Y. Shi and X. Xiao, "Facile spray-coating for fabrication of superhydrophobic SiO_2/PVDF nanocomposite coating on paper surface," *Journal of Dispersion Science and Technology*, vol. 37, no. 5, pp. 640–645, 2016.

[9] N. Wang, D. Xiong, S. Pan, Y. Deng, Y. Shi, and K. Wang, "Superhydrophobic paper with superior stability against deformations and humidity," *Applied Surface Science*, vol. 389, pp. 354–360, 2016.

[10] Y. Lu, S. Sathasivam, J. Song, C. R. Crick, C. J. Carmalt, and I. P. Parkin, "Repellent materials. Robust self-cleaning surfaces that function when exposed to either air or oil," *Science*, vol. 347, no. 6226, pp. 1132–1135, 2015.

[11] P. Dimitrakellis, A. Travlos, V. P. Psycharis, and E. Gogolides, "Superhydrophobic paper by facile and fast atmospheric pressure plasma etching," *Plasma Processes and Polymers*, vol. 14, no. 3, 2017.

[12] X. Zhong, J. Sheng, and H. Fu, "A novel UV/sunlight-curable anti-smudge coating system for various substrates," *Chemical Engineering Journal*, vol. 345, pp. 659–668, 2018.

[13] C. Zheng, G. Liu, and H. Hu, "UV-curable antismudge coatings," *ACS Applied Materials & Interfaces*, vol. 9, no. 30, pp. 25623–25630, 2017.

[14] X. Wu, M. Liu, X. Zhong et al., "Smooth water-based anti-smudge coatings for various substrates," *ACS Sustainable Chemistry & Engineering*, vol. 5, no. 3, pp. 2605–2613, 2017.

[15] M. Rabnawaz and G. Liu, "Graft-copolymer-based approach to clear, durable, and anti-smudge polyurethane coatings," *Angewandte Chemie International Edition*, vol. 54, no. 22, pp. 6516–6520, 2015.

[16] L. Jiang, Z. Tang, R. M. Clinton, D. W. Hess, and V. Breedveld, "Fabrication of highly amphiphobic paper using pulp debonder," *Cellulose*, vol. 23, no. 6, pp. 3885–3899, 2016.

[17] L. Li, V. Breedveld, and D. W. Hess, "Design and fabrication of superamphiphobic paper surfaces," *ACS Applied Materials & Interfaces*, vol. 5, no. 11, pp. 5381–5386, 2013.

[18] L. Jiang, Z. Tang, R. M. Clinton, V. Breedveld, and D. W. Hess, "Two-step process to create "roll-off" superamphiphobic paper surfaces," *ACS Applied Materials & Interfaces*, vol. 9, no. 10, pp. 9195–9203, 2017.

[19] P. Phanthong, G. Guan, S. Karnjanakom et al., "Amphiphobic nanocellulose-modified paper: fabrication and evaluation," *RSC Advances*, vol. 6, no. 16, pp. 13328–13334, 2016.

[20] D. Ge, L. Yang, C. Wang, E. Lee, Y. Zhang, and S. Yang, "A multi-functional oil–water separator from a selectively pre-wetted superamphiphobic paper," *Chemical Communications*, vol. 51, no. 28, pp. 6149–6152, 2015.

[21] J. Li, L. Yan, Q. Ouyang et al., "Facile fabrication of translucent superamphiphobic coating on paper to prevent liquid pollution," *Chemical Engineering Journal*, vol. 246, pp. 238–243, 2014.

[22] B. N. Sahoo, S. Nanda, J. A. Kozinski, and S. K. Mitra, "PDMS/camphor soot composite coating: towards a self-healing and a self-cleaning superhydrophobic surface," *RSC Advances*, vol. 7, no. 25, pp. 15027–15040, 2017.

[23] S. J. Yang, X. Chen, B. Yu, H. L. Cong, Q. H. Peng, and M. M. Jiao, "Self-cleaning superhydrophobic coatings based on PDMS and TiO_2/SiO_2 nanoparticles," *Integrated Ferroelectrics*, vol. 169, no. 1, pp. 29–34, 2016.